Electronic Supplementary Information (ESI)

Macrocyclic dinuclear, helical, layer and 3-D Ag(I) complexes constructed from AgX (X = NO_3^- and ClO_4^-) and flexible bis(pyridyl) ligands with chelating spacer: syntheses, structures and photoluminescence properties

Jing Huang, Zhao-Peng Deng, Ying-Hui Xiao, Li-Hua Huo*, Shu-Nan Zhao, Fa-Yuan Ge and Shan Gao*

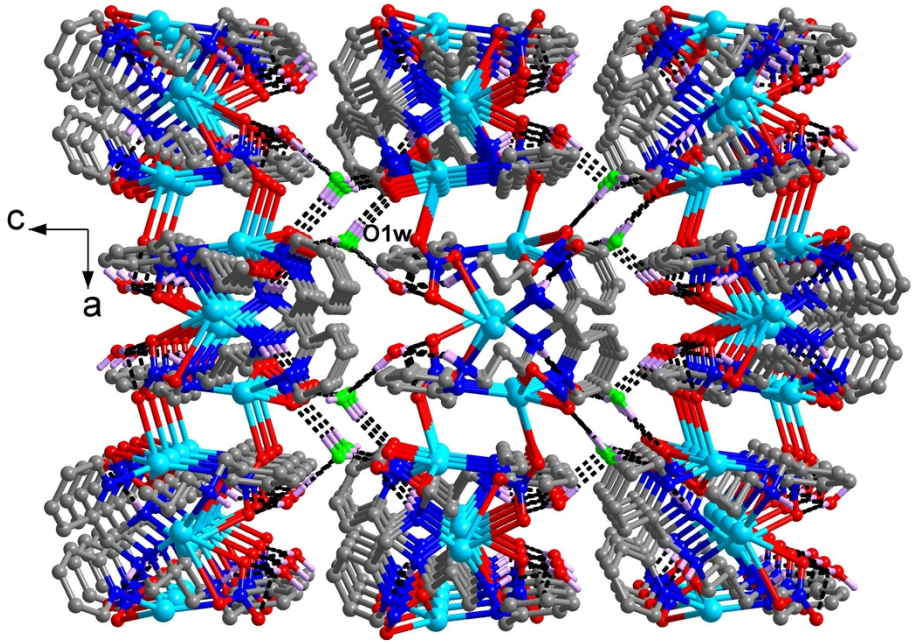

Fig. S1 3-D supramolecular network of **1** extended by the lattice water molecules (green balls).

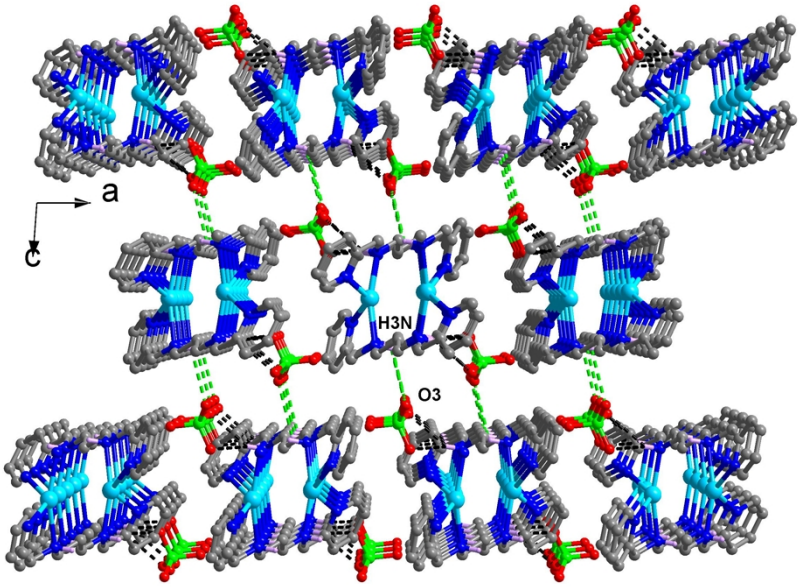

Fig. S2 3-D supramolecular network of **2** extended by hydrogen-bonding interactions (green dashed lines).

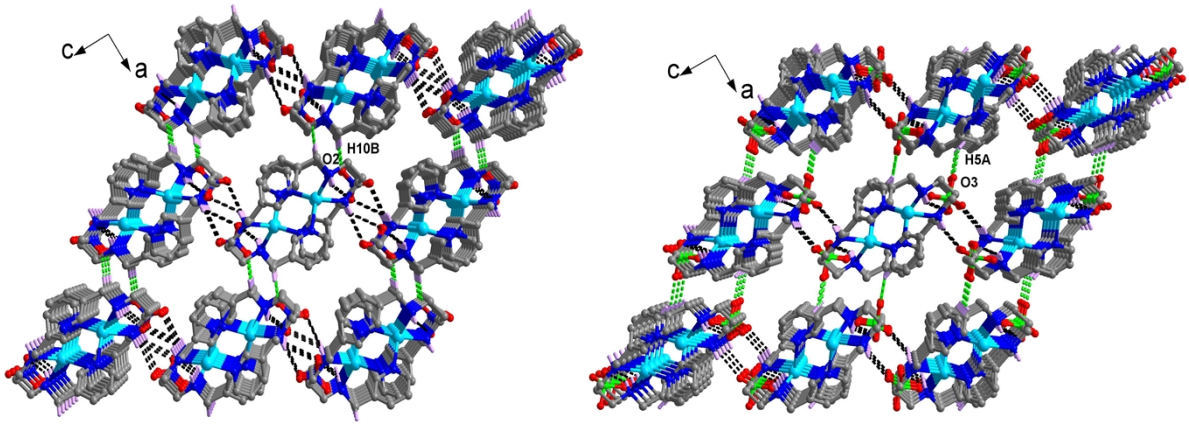

Fig. S3 3-D supramolecular networks of **3** (left) and **4** (right) extended by hydrogen-bonding interactions (green dashed lines).

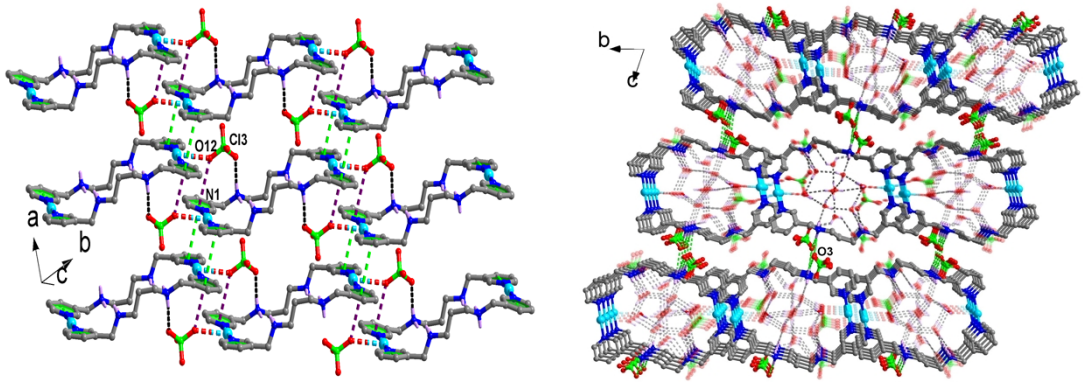

Fig. S4 Left: Extension of dinuclear units into layer motif through π···π (green dashed lines) and anion···π interactions (violet dashed lines). The hydrogen-bonding and weak Ag···O interactions were denoted as black and double-colored dash lines. Right: 3-D host-guest supramolecular network of **5** extended by hydrogen-bonding interactions (green dashed lines).

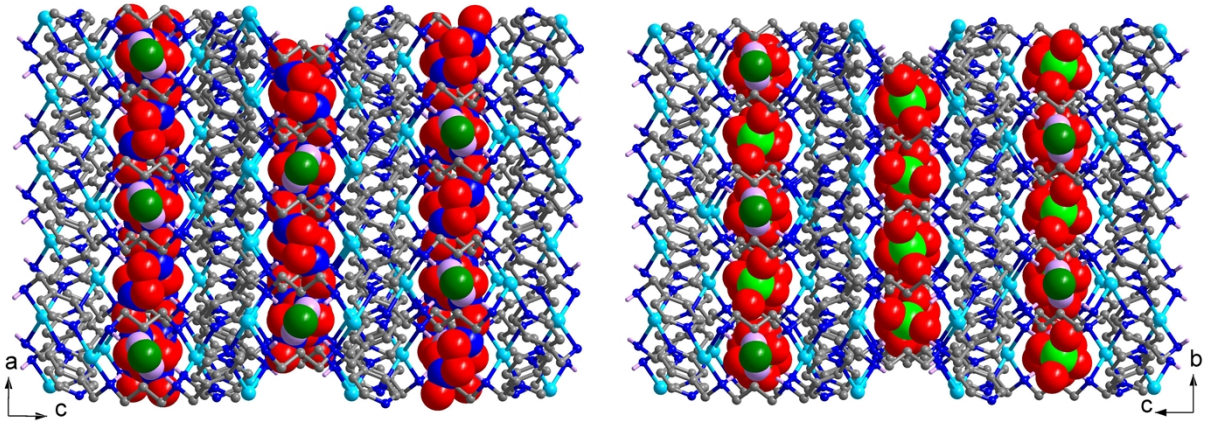

Fig. S5 3-D microporous networks of **6** (left) and **7** (right) showing the small channels along *b*- or *a*-axis. The guest anions and water molecules were denoted as space-filling modes.

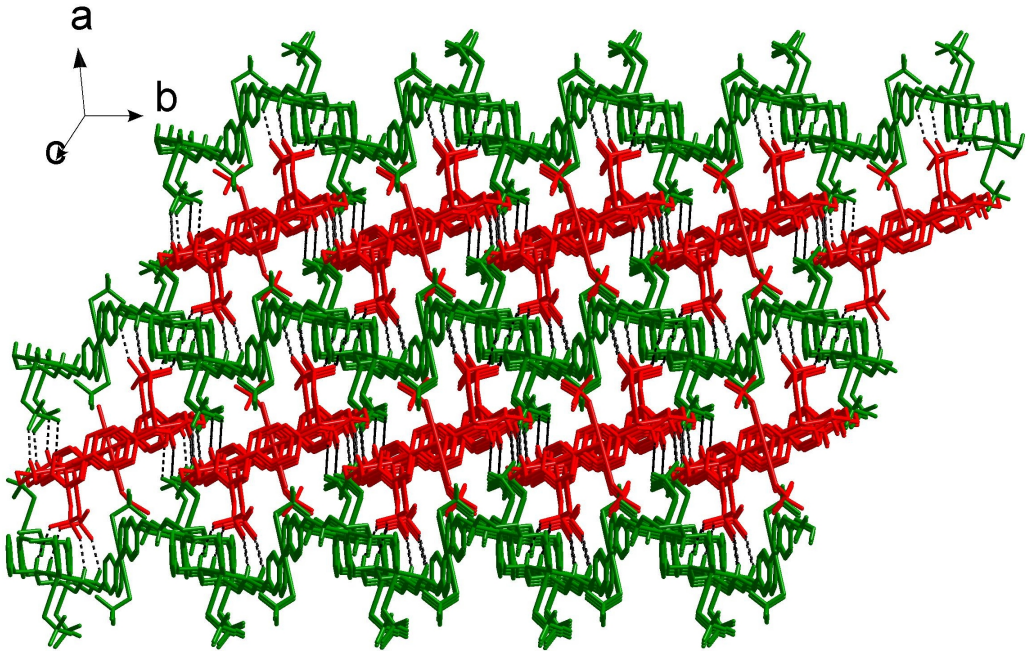

Fig. S6 3-D supramolecular network of **8** extended by hydrogen-bonding interactions (black dashed lines). Green and red lines indicated the snake-shaped chains in different directions.

Powder X-ray diffraction (PXRD)

Powder X-ray diffraction (PXRD) patterns for solid samples of complexes **1-8** are measured at room temperature as illustrated in Fig. S7. The patterns are highly similar to their simulated ones (based on the single-crystal X-ray diffraction data), indicating that the single-crystal structures are really representative of the bulk of the corresponding samples.

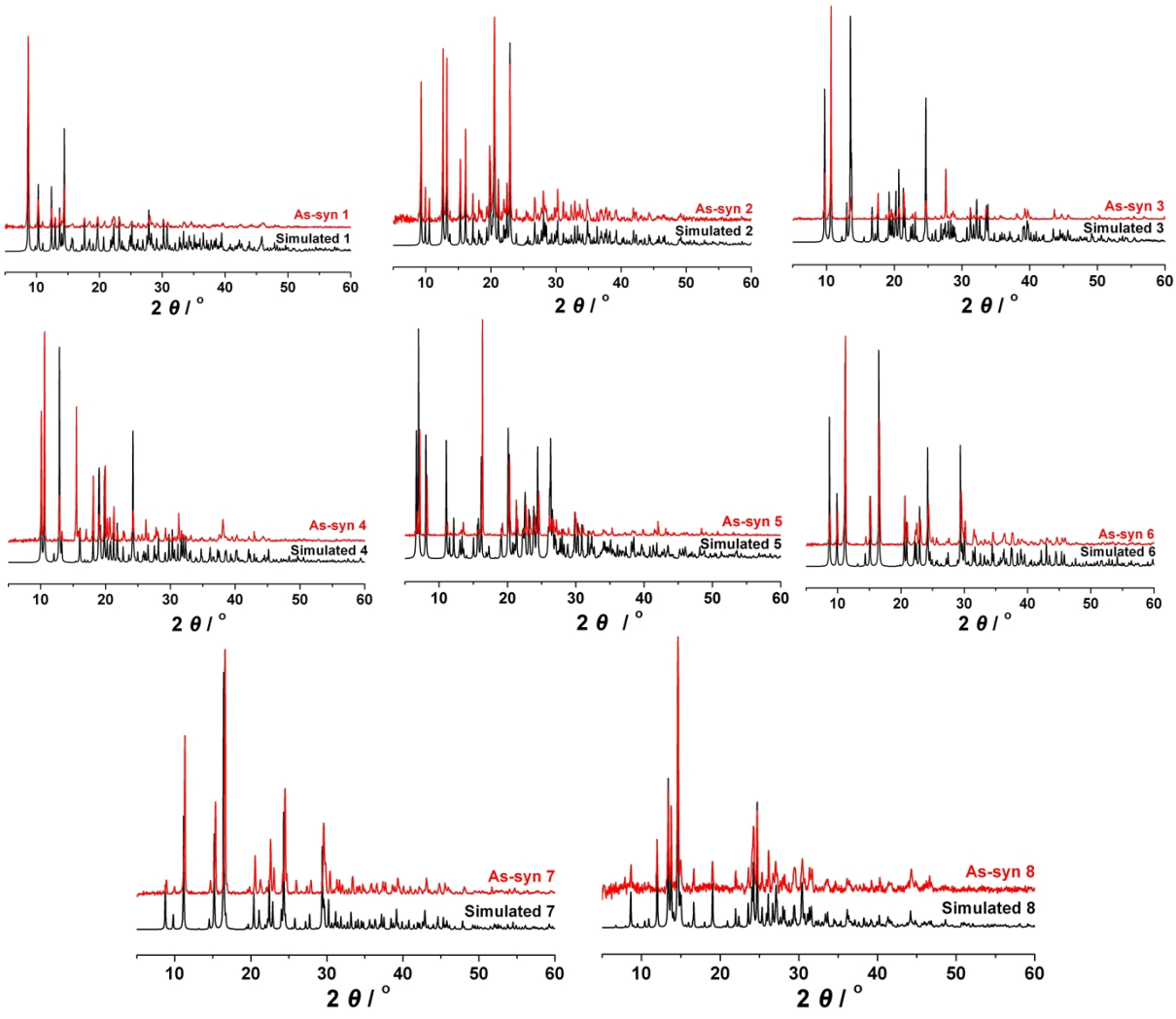

Fig. S7 PXRD patterns for complexes **1**-**8**.

Thermogravimetric analysis (TGA)

The thermal stability of complexes **1-8** were analyzed on crystalline samples by thermogravimetric analyses (TGA) from room temperature to 900 °C at a rate of 10 °C min^{-1} under N_2 atmosphere. As shown in Fig. S8, the TGA curves indicate that complexes **1** and **5-7** show two loss steps with the first one corresponding to the release of lattice water molecules during the range 60-122 °C for **1**, 59-130 °C for **5**, 50-102 °C for **6** and 62-112°C for **7**, respectively. The observed weight loss of 5.64% in **1**, 10.94% in **5**, 4.11% in **6** and 3.78% in **7**, are reasonably close to the calculated value (5.70% in **1**, 10.86% in **5**, 4.06% in **6** and 3.74% in **7**). Then, the organic components are removed progressively, leaving the residual of Ag at 736 °C for **1**, 336 °C for **5**, 754 °C for **6** and 847 °C for **7**, respectively. In contrast to the above four complexes, complexes **2-4** and **8** undergo a slow weight loss during the range 185-850 °C for **2**, 190-870 °C for **3**, 210-790 °C for **4** and 180-825°C for **8**, respectively, and also leaving the residual of Ag. All the left values for the residual of Ag (34.21% for **1**, 23.30% for **2**, 25.45% for **3**, 23.37% for **4**, 14.55% for **5**, 24.41% for **6**, 22.53% for **7**, and 28.62% for **8**) are close to

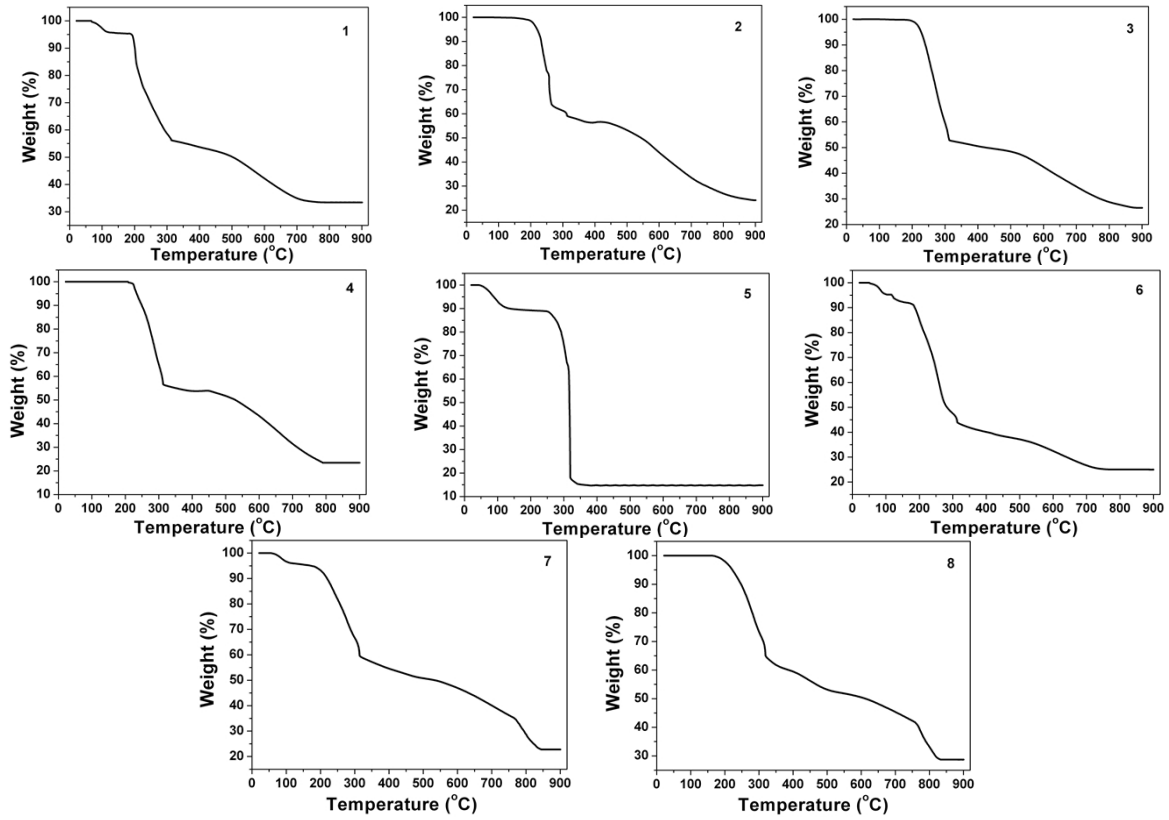

Fig. S8 TG curves of complexes **1-8**

their calculated values (34.13% for **1**, 23.26% for **2**, 25.31% for **3**, 23.26% for **4**, 14.45% for **5**, 24.28% for **6**, 22.40% for **7**, and 28.52% for **8**).

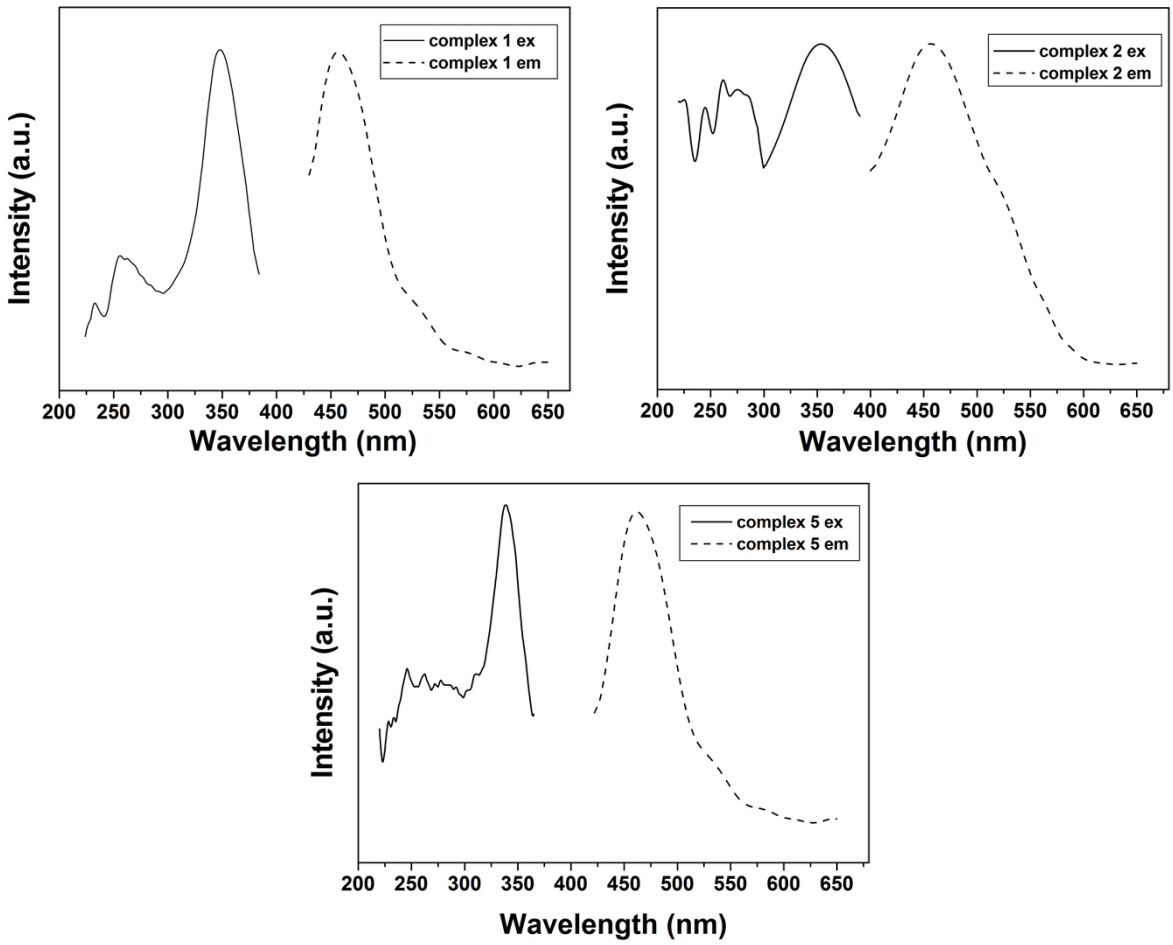

Fig. S9 Excitation and emission spectra of complexes **1**, **2** and **5** in solid state at room temperature.

Table S1 Selected bond distances (Å) for complexes **1**-**8**[a]

Complex **1**			
Ag(1)-N(1)	2.228(4)	Ag(1)-Ag(2)	3.0163(5)
Ag(1)-N(4)^{i}	2.272(4)	Ag(2)-N(3)^{i}	2.215(4)
Ag(1)-O(4)	2.551(4)	Ag(2)-N(2)	2.215(3)
Ag(1)-O(1)	2.571(5)		
Complex **2**			
Ag(1)-N(2)	2.264(4)	Ag(1)-N(4)^{i}	2.368(4)
Ag(1)-N(3)^{i}	2.345(4)	Ag(1)-N(1)	2.454(4)
Complex **3**			
Ag(1)-N(1)	2.283(3)	Ag(1)-N(2)^{i}	2.367(3)
Ag(1)-N(3)^{i}	2.358(3)	Ag(1)-N(4)^{ii}	2.369(3)
Complex **4**			
Ag(1)-N(1)	2.268(4)	Ag(1)-N(2)^{i}	2.399(4)
Ag(1)-N(3)^{i}	2.363(4)	Ag(1)-N(4)^{ii}	2.419(4)
Complex **5**			
Ag(1)-N(4)^{i}	2.137(4)	Ag(1)-N(1)	2.144(4)
Complex **6**			
Ag(1)-N(1)^{i}	2.357(7)	Ag(1)-N(2)^{ii}	2.421(6)
Ag(1)-N(1)	2.357(7)	Ag(1)-N(2)^{iii}	2.421(6)
Complex **7**			
Ag(1)-N(1)	2.384(5)	Ag(1)-N(2)^{ii}	2.400(4)
Ag(1)-N(1)^{i}	2.384(5)	Ag(1)-N(2)^{iii}	2.400(4)
Complex **8**			
Ag(1)-N(1)	2.128(5)	Ag(3)-N(4)	2.202(5)
Ag(1)-N(1)^{i}	2.128(5)	Ag(3)-N(7)	2.318(5)
Ag(2)-N(5)	2.221(5)	Ag(3)-N(6)	2.341(5)
Ag(2)-N(2)	2.343(5)	Ag(4)-N(8)^{ii}	2.138(6)
Ag(2)-N(3)	2.365(5)	Ag(4)-N(8)	2.138(6)

[a]Symmetry tansformations used to generate equivalent atoms: For **1** (i) -x+3/2,y+1/2,z; For **2** (i) -x+3/2,y+1/2,-z+3/2; For **3** (i) -x+1,-y+1,-z+1; (ii) x,y+1,z; For **4** (i) -x+1,-y+1,-z+1; (ii) x,y-1,z; For **5** (i) -x+2,-y+1,-z+1; For **6** (i) -x+3/4,-y+3/4,z; (ii) x-1/4,y+1/4,-z+1/2; (iii) -x+1,-y+1/2,-z+1/2; For **7** (i) -x-3/4,-y-3/4,z; (ii) x-1/4,y-1/4,-z; (iii) -x-1/2,-y-1/2,-z; For **8** (i) -x+1,-y-1,-z; (ii) -x,-y,-z-1.

Table S2 Selected hydrogen bond parameters for complexes **1-8**[a]

D-H...A	d(D-H)	d(H...A)	d(D...A)	<(DHA)
Complex **1**				
O(1W)-H(1W1)...O(3)^{iii}	0.85	1.99	2.826(8)	166.8
O(1W)-H(1W2)...O(1)	0.85	1.86	2.698(7)	167.3
O(1W)-H(1W2)...O(3)	0.85	2.51	3.176(7)	136.3
O(2W)-H(2W1)...O(1W)	0.85	1.74	2.589(9)	172.3
O(2W)-H(2W2)...O(6)	0.85	2.17	3.011(7)	171.6
O(2W)-H(2W2)...O(4)	0.85	2.42	3.055(7)	131.9
N(2)-H(2N)...O(2W)^{iv}	0.85(4)	2.21(2)	3.003(6)	154(4)
N(3)-H(3N)...O(3)^{v}	0.86(4)	2.269(15)	3.114(6)	168(4)
N(3)-H(3N)...O(2)^{v}	0.86(4)	2.56(3)	3.265(6)	140(4)
Complex **2**				
N(2)-H(2N)...O(1)	0.86(8)	2.49(4)	3.217(8)	144(5)
N(2)-H(2N)...O(2)	0.86(8)	2.53(2)	3.349(8)	161(5)
N(3)-H(3N)...O(3)^{iii}	0.86(1)	2.84(1)	3.288(1)	114(2)
Complex **3**				
N(2)-H(2N)...O(3)^{iv}	0.86(5)	2.408(12)	3.264(5)	178(4)
N(2)-H(2N)...O(1)^{iv}	0.86(5)	2.63(3)	3.260(5)	131(3)
N(3)-H(3N)...O(1)	0.86(5)	2.35(2)	3.140(5)	154(4)
Complex **4**				
N(2)-H(2N)...O(4)	0.85(3)	2.45(3)	3.28(3)	162(5)
N(3)-H(3N)...O(1)^{iv}	0.86(3)	2.43(3)	3.173(9)	145(5)
Complex **5**				
O(1W)-H(1W1)...O(11)^{ii}	0.85	2.31	3.143(7)	168.5
O(1W)-H(1W2)...O(2W)	0.85	1.95	2.786(11)	169.2
O(2W)-H(2W1)...O(6)	0.84(4)	2.34(4)	2.976(9)	134(5)
O(2W)-H(2W2)...O(2)	0.84(4)	2.41(4)	3.016(11)	131(5)
O(3W)-H(3W1)...O(4W)	0.85	2.01	2.853(6)	170.4
O(3W)-H(3W2)...O(11)^{iii}	0.85	2.17	3.014(6)	170.1
O(4W)-H(4W1)...O(1W)	0.85	1.87	2.681(9)	159.7
O(4W)-H(4W2)...O(5W)	0.85	2.09	2.902(6)	160.3

O(5W)-H(5W1)...O(3W)[i]	0.85	1.98	2.826(6)	172.3
O(5W)-H(5W2)...O(7)[i]	0.85	2.19	3.033(7)	172.2
N(2)-H(2N2)...O(5W)[i]	0.86(2)	2.08(2)	2.898(5)	160(4)
N(2)-H(2N1)...O(9)[iii]	0.86(2)	2.25(2)	3.022(6)	150(4)
N(2)-H(2N1)...O(6)[iii]	0.86(2)	2.53(4)	3.141(8)	129(4)
N(3)-H(3N1)...O(3)	0.86(2)	2.37(2)	3.187(8)	156(4)
N(3)-H(3N1)...O(3)[iv]	0.86(2)	2.38(3)	3.014(7)	130(4)
N(3)-H(3N2)...O(4W)[i]	0.86(2)	2.03(2)	2.844(6)	156(4)
Complex **6**				
O(1W)-H(1W)...O(1)	0.85	2.04	2.870(15)	172.0
N(2)-H(2)...O(1W)	0.88	2.17	3.050(8)	175.2
Complex **7**				
O(1W)-H(1W)...O(1)	0.85	2.42	3.13(2)	142.0
N(2)-H(2N)...O(1W)	0.86(7)	2.313(13)	3.172(7)	175(5)
Complex **8**				
N(2)-H(2N)...O(8)[iii]	0.86(3)	2.28(3)	3.088(6)	156(6)
N(3)-H(3N)...O(6)[iii]	0.86(3)	2.47(3)	3.246(7)	150(6)
N(6)-H(6N)...O(3)[iv]	0.86(3)	2.39(3)	3.200(8)	157(6)
N(7)-H(7N)...O(4)[iv]	0.86(3)	2.36(4)	3.089(7)	143(6)

[a]Symmetry transformations used to generate equivalent atoms: For **1**, (iii) -x+1,-y+2,-z+2; (iv) -x+1,y-1/2,-z+3/2; (v) x,y-1,z; For **2**, (iii) -x+1,-y+1,-z+1; For **3**, (iv) -x+1/2,y+1/2,-z+3/2; For **4**, (iv) -x+3/2,y+1/2,-z+1/2; For **5**, (i) -x+2,-y+1,-z+1; (ii) -x+1,-y+1,-z+1; (iii) x+1,y,z; (iv) -x+2,-y+1,-z+2; For **8**, (iii) -x,y-1/2,-z-1/2; (iv) -x+1,y+1/2,-z-1/2.

Table S3 Detailed structural analyses of complexes **1**-**8**

complexes	coordination modes	conformations	metal geometry	structures
1	μ_4 (κ^1N1 : κ^1N2 : κ^1N3 : κ^1N4)	distorted 'W' shaped	N_2O_2Ag tetradrons	(4,4) layer
			N_2OAg triangles	
2	μ_2 (κ^1N1 : κ^1N2 : κ^1N3 : κ^1N4)	linear	N_4Ag tetrahedra	helix
3	μ_3 (κ^1N1 : κ^1N2 : κ^1N3 : κ^1N4)	'V' shaped	N_4Ag tetrahedra	helix
4	μ_3 (κ^1N1 : κ^1N2 : κ^1N3 : κ^1N4)	'V' shaped	N_4Ag tetrahedra	helix
5	μ_2 (κ^1N1 : κ^1N4)	'L' shaped	N_2Ag lines	dinuclear
6	μ_4 (κ^1N1 : κ^1N2 : κ^1N3 : κ^1N4)	'W' shaped	N_4Ag tetrahedra	3D network
7	μ_4 (κ^1N1 : κ^1N2 : κ^1N3 : κ^1N4)	'W' shaped	N_4Ag tetrahedra	3D network
8	μ_3 (κ^1N1 : κ^1N2 : κ^1N3 : κ^1N4)	'V' shaped	N_3OAg tetrahedral	snake-shaped
	μ_3 (κ^1N5 : κ^1N6 : κ^1N7 : κ^1N8)		N_3Ag triangles	chain
			N_2Ag lines	